

Estimation of the nonlinearity of the surface soil at Tsukidate during the 2011 off the Pacific coast of Tohoku Earthquake

Takashi Hayakawa, Toshimi Satoh & Mitsutaka Oshima

SHIMIZU Corporation, Japan

Hiroshi Kawase & Shinichi Matsushima

DPRI, University of Kyoto, Japan

Baoyintu, Fumiaki Nagashima & Kenichi Nakano

Graduate School of Engineering, University of Kyoto, Japan



SUMMARY:

At Tsukidate K-NET station (MYG004), very large acceleration ($> 0.5G$) with long duration for more than several tens of seconds has been observed during the 2011 off the Pacific coast of Tohoku Earthquake (M9.0). In this study, we estimated the 1D velocity structure beneath MYG004 based on the microtremor measurements and the site response by spectral inversion. Using the estimated structure, we did simulations of the strong ground motions by equivalent linear method. The stress-strain and damping-strain relations have been estimated by fitting the predominant frequencies of theoretical S wave amplification to those of the large acceleration records during the main shock and several other large earthquakes. From reproduction of decreasing predominant frequencies of S-wave amplification, stress-strain and damping-strain relations of the shallow (about 10m) surface soil is within -1 and +1 sigma of relations by previous studies (Imazu et al, 1986) respectively.

Keywords: the 2011 off the Pacific coast of Tohoku Earthquake, nonlinearity of soil, equivalent linear method

1. INTRODUCTION

At Tsukidate K-NET station (MYG004), which is in Miyagi Prefecture Japan and about 50km away from the source region of the 2011 off the Pacific coast of Tohoku Earthquake (Mw9.0), very large acceleration ($> 0.5G$) with long duration for more than several tens of seconds has been observed during the main shock. In this study, we estimate the 1D velocity structure beneath MYG004 based on the microtremor measurements and the site response by spectral inversion. And then we considered the nonlinearity of the surface layers by the simulations of the strong ground motions during the main shock.

2. ESTIMATION OF 1D VELOCITY STRUCTURE AT MYG004

2.1. Microtremor Array Measurements

We did microtremor array measurements in the parking lot near MYG004 station. Figure 1 shows the array. Length of the array is 66m and 100m in NS and EW direction respectively. Centre of the array is away from about 50m from MYG004.

We calculate FK power spectra at 1.5, 2.0, 2.5, 3.0, 4.2, 5.0, 5.5, 6.0, 6.2 and 6.5Hz from vertical component of microtremor with 18 minutes duration by the high resolution method (Capon, 1973). We estimate the phase velocities of Rayleigh waves from the wave number at maximum FK power spectra. FK power spectra has clear peaks in each frequency and the phase velocities are dispersive, we think phase velocities of Rayleigh waves are estimated successfully. In the frequency range below 1.5Hz, FK power spectra become flat and we don't estimate phase velocities. At the site away from several kilometres from MYG004, the phase velocities in the frequency range below 1.0Hz were

estimated from microtremor by SPAC (Fukumoto et al, 2007) . We assume that deep velocity structure, which affects phase velocity in such low frequency, is not much different between their site and the parking lot. We use phase velocities estimated by them in the frequency range below 1.0Hz. In the frequency range above 6.5Hz, aliasing appears in FK power spectra and we don't estimate. The left figure in Figure 2 shows the phase velocities from microtremor at the parking lot.



Figure 1. Microtremor array in the parking lot near MYG004

2.2. Estimation of 1D Velocity Structure Near MYG004

We estimate 1D velocity structure at the parking lot by fitting theoretical dispersion curve of fundamental Rayleigh mode to the phase velocities of microtremor. We use quasi-Newton method. The 24 initial models are made to find a global solution. At first, the average initial model is made by embedding the velocity structure by PS logging at MYG004 in the velocity structure estimated down to seismological basement by Fukumoto et al (2007) near MYG004. And then we add 24 random fluctuations whose coefficient of variation is 0.2 to the average initial model.

In the fitting, we optimize S-wave velocities of all layers and fix thicknesses of layers. P-wave velocity is connected with S-wave velocity using the empirical relation (Kitsunozaki et al, 1990). The 24 optimized models are obtained. We choose the best optimized model provided that 1) sum of residual $|\text{Obs.}(f)-\text{Cal.}(f)|/\text{Cal.}(f)$ is small, 2) theoretical ellipticity of Rayleigh waves predominate at 5Hz as H/V spectra of microtremor predominate. The best optimized model (call the parking model here after) is listed in Table 2.1. The left figure in Figure 2 is comparison of dispersion curve of the parking model and phase velocities of microtremor. The right figure is same as left figure but H/V spectra. H/V spectra calculated from the parking model reproduce predominance at 5Hz of microtremor.

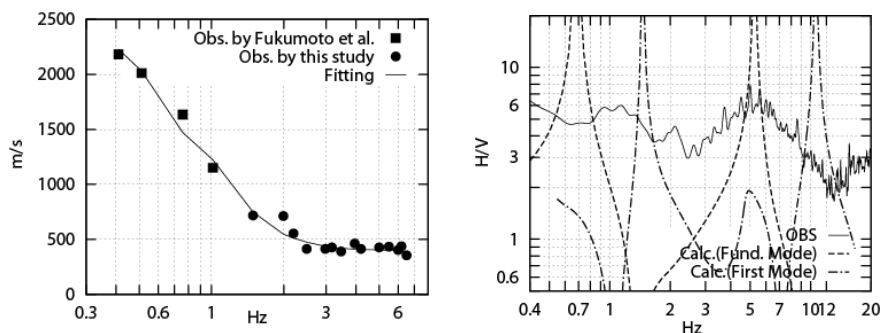


Figure 2. Comparison of dispersion curve(left) and H/V spectra(right) between microtremor and theory of the parking model

2.3. Estimation of 1D Velocity Structure at MYG004

At MYG004, the site response was estimated by the spectral inversion (Sato, 2006a) in the frequency range up to 4Hz. In this study, we expand frequency of the site response to 12Hz by changing the reference site where the 1D velocity structure was estimated up to 12Hz. The reference site is changed to top of the layer whose S-wave velocity is 2630m/s at KiK-net MYGH03.

S-wave amplification from top of 3rd and 8th layer in the optimized model are shown in Figure 4. We used Q value evaluated in Sendai city (Sato, 2006b). The site response is also plotted in this Figure. the site response predominant at 4Hz and 10Hz. But S-wave amplification of the optimized model predominant at 5Hz, 13Hz and is higher than the site response.

Predominance of S-wave amplification at 5Hz and 10Hz are generated by 1st and 2nd layers. So we modify S-wave velocities (Case-A) or thickness (Case-B) of 1st and 2nd layers to match predominant frequencies of the site response. In Case-A, we decrease S-wave velocity to 80%. In Case-B, we increase thickness to 120%. S-wave amplification of Case-A and Case-B are shown in Figure 3. Both cases reproduce predominance at 4Hz and 10Hz of the site response. Close to MYG004, we did small microtremor array measurement (The left figure in Figure 4). Diameter of the small array is about 20m. We calculate FK power spectra at 10, 11, 12Hz. Phase velocities of microtremor in the small array and dispersion curves of Case-A and Case-B is shown in the right figure in Figure 4. Case-B is better in agreement with the phase velocities of microtremor. We use the velocity model in Case-B in the following chapters.

Table 2.1. Velocity Structure at MYG004

Layer	Dens. (g/cc)	Damping (5Hz)	P-wave Velocity(m/s)			S-wave velocity(m/s)			Thickness(m)		
			Parking	CaseA	CaseB	Parking	CaseA	CaseB	Parking	CaseA	CaseB
1	1.8	0.073	1453	1420	1453	147	117	147	5	←	6
2	1.8	0.073	1510	1466	1510	199	159	199	5	←	6
3	2.0	0.033	1860	←	←	514	←	←	20	←	←
4	2.0	0.033	1766	←	←	429	←	←	50	←	←
5	2.0	0.033	2016	←	←	654	←	←	140	←	←
6	2.3	0.012	3056	←	←	1591	←	←	320	←	←
7	2.3	0.012	3398	←	←	1899	←	←	660	←	←
8	2.6	0.007	4620	←	←	3000	←	←	Inf.	←	←

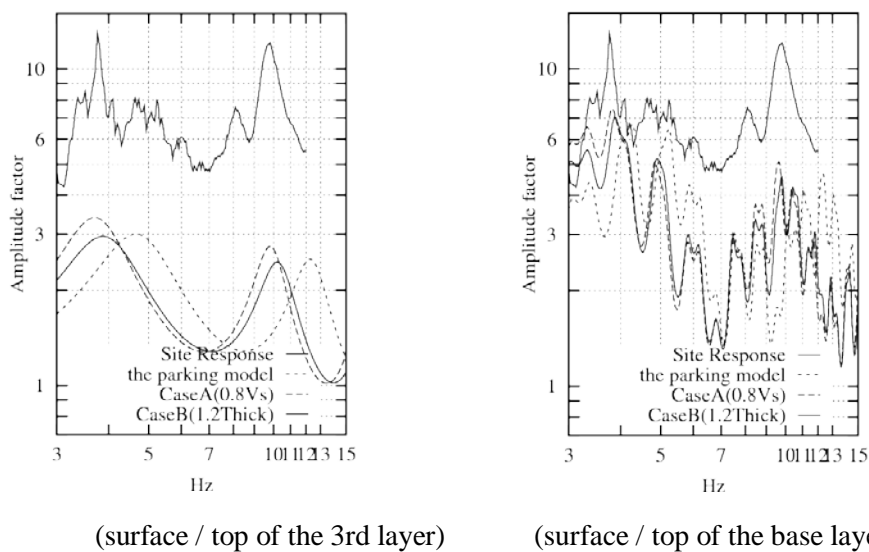


Figure 3. The Site response at MYG004 and S-wave amplification of the parking model, Case-A and Case-B

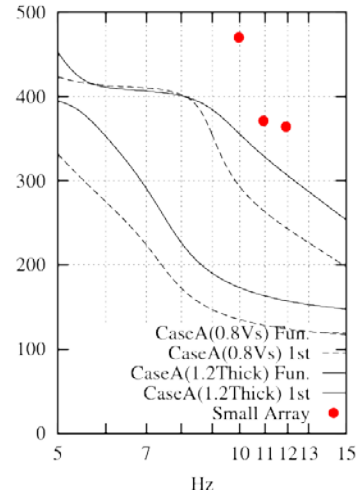


Figure 4. The small microtremor array close to MYG004 (left) phase velocities of microtremor in the small array and dispersion curve of Case-A Case-B (right)

3. NONLINER CHARACTERISTICS OF THE SURFACE SOIL

In addition to the 2011 off the Pacific coast of Tohoku Earthquake (call the Tohoku Earthquake here after), strong ground motions during the large earthquakes, the 2008 Iwate-Miyagi Nairiku Earthquake, the 2005 off Miyagi Prefecture Earthquake, the 2003 northern Miyagi, were observed at MYG004. Figure 5 shows these large earthquakes. We identify predominant peaks caused by S-wave amplification of sediments, whose frequencies were decreased due to nonlinearity of the soil, from spectra ratio of EW and UD component. Imazu et al (1986) proposed the average and standard deviation of nonlinearity characteristics by many studies. Using the average and standard deviation of nonlinear characteristics, we did simulations of strong ground motions during the Tohoku Earthquake and the large earthquakes by equivalent liner method and investigated the nonlinearity of the surface soil at MYG004.

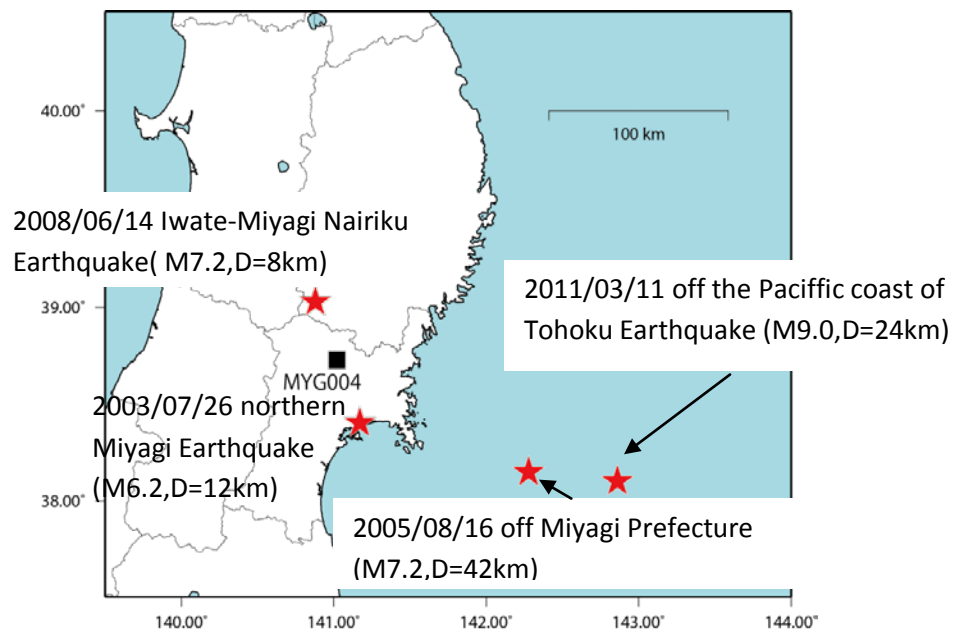


Figure 5. The Tohoku Earthquake and the large earthquakes used in this study

3.1. Predominant Frequencies of S-wave Amplification During the Tohoku Earthquake and Several Large Earthquakes

Particle motions on NS-UD and EW-UD sections during the Tohoku Earthquake are shown in Figure 6. In frequency range above 4Hz, convex arc-shaped orbit are recognized in all time of NS-UD section and the second half time of EW-UD section. Rocking of the basement of the seismometer might be a reason. We use only the first half time of records in EW and UD directions. In the same way, we used the records of EW and UD component in the other earthquakes.

Fourier spectra of EW and UD records and its ratio (EW/UD) are shown in Figure 7. Strong ground motions during the Tohoku Earthquake (Max.=958 cm/s/s) is largest among all. The Iwate-Miyagi Nairiku Earthquake (Max.=678cm/s/s) is 2nd, the off Miyagi Prefecture Earthquake (Max.=381cm/s/s) is 3rd, the northern Miyagi (349cm/s/s) is 4th. We identify the predominant peaks, which correspond to the predominant peaks at 4Hz and 10Hz in the site response, in spectra ratio of each earthquake. In identifying peaks, we make conditions that 1) frequencies of peaks decrease in order of amplitude of strong ground motion 2) peaks are high. Identified peaks and their frequencies are shown in Figure 8 and Table 3.1. In Figure 7, the peaks corresponding 4Hz and 10Hz in the site response are marked by black and white triangles respectively. In the northern Miyagi earthquake and the Iwate-Miyagi Nairiku Earthquake, a peak corresponding to 4Hz can not be identified. If vertical motions on ground surface are consisted from P-wave converted at boundary between sediment and seismological basement from SV wave and sediments do not amplify P-wave, spectra ratio of horizontal to vertical motions are S-wave amplification by sediments. Inversely if amplification of P-wave has peaks, it is difficult to find predominant peaks by S-wave amplification in spectra ratio. Amplification of P-wave probably has a peak at 2Hz because fourier spectra of the all earthquakes have a peak at 2Hz. Because of the peak, it probably predominant peaks by S-wave amplification are not clearly seen around 2Hz. In the Tohoku Earthquake, there is a weak peak at 2Hz in spectra ratio and a clear peak in fourier spectra of EW component (black square in Figure 7) at 2Hz. We think the predominant peak at 2Hz is a peak by S-wave amplification.

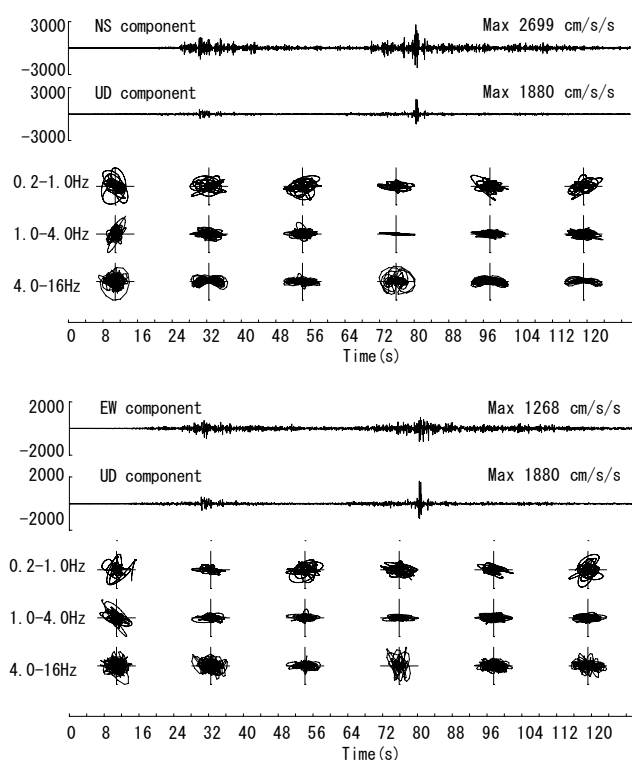


Figure 6. Particle motion during the Tohoku Earthquake at MYG004

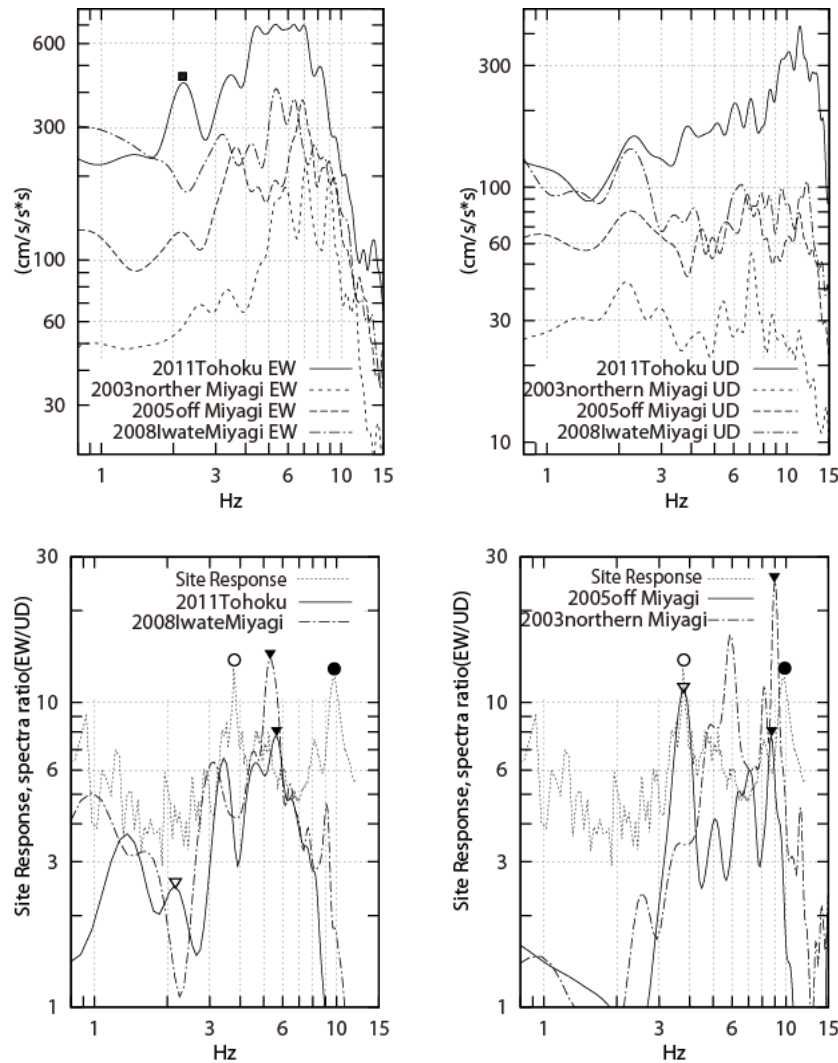


Figure 7. Fourier spectra of EW, UD component and spectra ratio (EW/UD)

3.2. Simulations of Strong Ground Motions by Equivalent Linear Method

The strong ground motions simulations are done by equivalent linear method. Predominant S-wave amplification at 4Hz and 10Hz in the site response are caused by mainly 1st and 2nd layers. Nonlinearity of these layers cause decreasing predominant frequency of S-wave amplification. Imazu et al (1986) proposed the average and standard deviation of stress-strain and damping-strain relation by many studies. In the simulations, we assign average(Case-1), strong(Case-2) and weak(Case-3) nonlinearity to 1st and 2nd layers and investigate which nonlinearity reproduce the decreased predominant frequencies of S-wave amplification.

Case1: average nonlinearity

Case2: strong nonlinearity (stress-strain relation : av.-sigma, damping-strain relation : av.+sigma)

Case3: weak nonlinearity(stress-strain relation : av.+sigma, damping-strain relation : av.-sigma)

Case4: linear

We assume clay for 1st and 2nd layers according to geological investigation around MYG004 (Fukumoto et al, 2007). Nonlinearity of sedimentary rock (Fujikawa,2001) is assigned from 3rd layer to 7th layers. We don't account nonlinearity in the base layer. The stress-strain and damping-strain relations used in this study are shown in Figure 8. Theoretical S-wave amplification rapidly decrease with frequency and is different from spectra ratio. We accounted dependency on frequency in the damping-strain relation. Dependency on frequency of Q is estimated as $f^{0.63}$ in Sendai (Satoh, 2006b). We think damping-stress relation by Imazu et al (1986) represent one at 5Hz and multiply $f^{0.63}/5^{0.63}$ to the damping-strain relation. When strain is low and damping becomes less than the one by Satoh

(2006b), we set damping by Satoh (2006b).

In each earthquake, S-wave amplifications from top of 3rd layer were compared between each case in Figure 9. Predominant frequencies in all cases are listed in Table 3.1. We calculate average predominant frequencies ratio of simulations and spectra ratio. In Case-1, predominant frequencies of simulations are higher than spectra ratio in average. On the other hand, Case2 is lower. Nonlinearity at MYG004 is thought to be middle of Case-1 and Case-2.

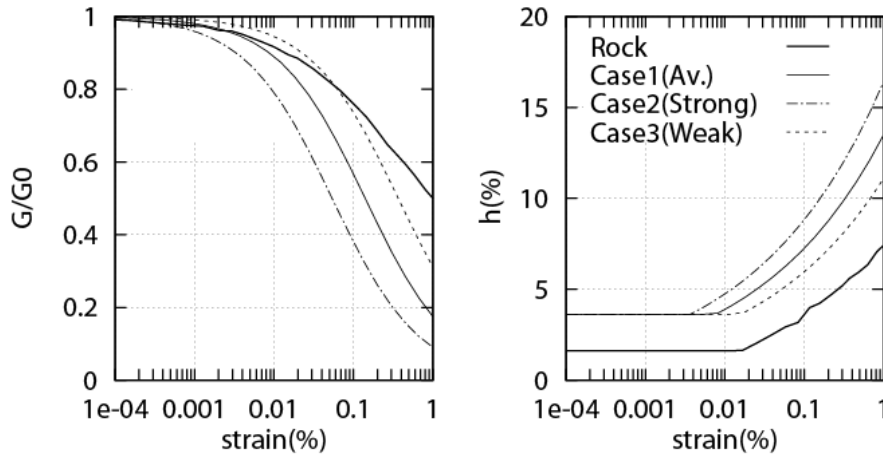


Figure 8. Stress-strain and damping-strain relation used in this study

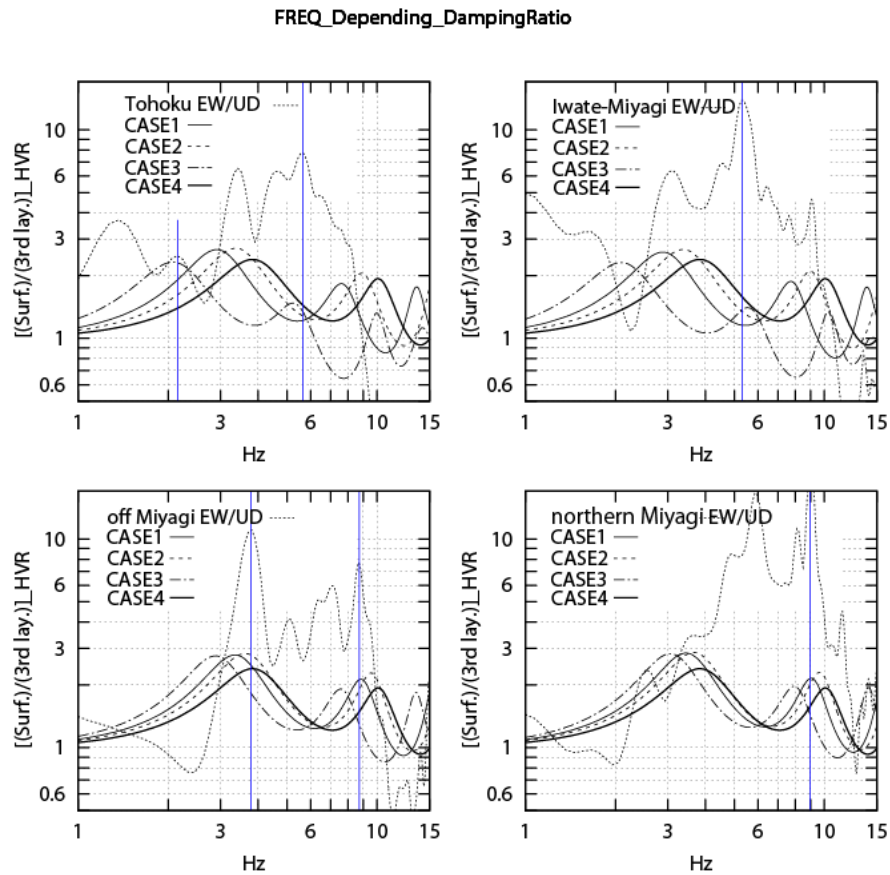


Figure 9. Comparison of S-wave amplification of simulations and spectra ratio

Table 3.1. Predominant frequencies of EW/UD spectra ratio and calculated predominant frequencies

	Earthquake	Peak coressponfing the 4Hz peak in the site response			Peak coressponfing the 10Hz peak in the site		
		Cal. (Hz)	Obs.(Hz)	Cal./Obs.	Cal. (Hz)	Obs.(Hz)	Cal./Obs.
Case1 (Average nonlinearity)	Tohoku	2.89	2.16	1.34	7.63	5.66	1.35
	Iwate-Miyagi Nairiku				9.05	8.96	1.01
	off Miyagi Pref.	3.33	3.78	0.88	8.85	8.73	1.01
	north Miyagi				7.73	5.32	1.45
	Average			1.11			1.21
Case2 (strong nonlinearity)	Tohoku	2.06	2.16	0.96	5.24	5.66	0.93
	Iwate-Miyagi Nairiku				7.92	8.96	0.88
	off Miyagi Pref.	2.89	3.78	0.77	7.58	8.73	0.87
	north Miyagi				5.53	5.32	1.04
	Average			0.86			0.93
Case3 (weak nonlinearity)	Tohoku	3.38	2.16	1.57	8.90	5.66	1.57
	Iwate-Miyagi Nairiku				9.63	8.96	1.08
	off Miyagi Pref.	3.63	3.78	0.96	9.53	8.73	1.09
	north Miyagi				9.00	5.32	1.69
	Average			1.26			1.36

4. CONCLUSION

Using the velocity structure estimated from microtremor and the site response at MYG004, we did simulations of strong ground motions at MYG004 during the 2011 off the Pacific coast of Tohoku Earthquake and other three large earthquakes by equivalent liner method. From reproduction of decreasing predominant frequencies of S-wave amplification, stress-strain and damping-strain relations of the shallow (about 10m) surface soil is within -1 sigma and +1 sigma of relations by previous studies (Imazu et al, 1986) respectively.

AKCNOWLEDGEMENT

This research was supported by JST on J-RAPID "Quantitative assessment of nonlinear soil response during the great Tohoku earthquake" (P.I. Prof. Kawase).

REFERENCES

- Capon, J.(1973). Signal Processing and Frequency-Wavenumber Spectrum Analysis for Large Aperture Seismic Array Method in *Computational Physics* **13**, 1-58.
- Fujikawa, S., Hayashi, Y. and Fukutake, K. (2001). The Effect of The Nonlinearity of Diluvial Deposite and Deep Sediment on The Eartquake Responses of Surface Ground and Buildings *J. Struct. Constr. Eng. AIJ* **545**, 71-77.
- Fukumoto, S., Unno, T., Sento, N., Uzuoka, R. and Kazama, M. (2007). Estimation of Strong Ground Motions at Tsukidate Landslide Site during the 2003 Sanriku-Minami Earthquake — Realization of Ground Motion Waveforms using the data of Strong Motion Seismometers and SeismicIntensity and Its Fluidization Mechanism using Laboratory Testing —. *Journal of Japan Association for Eartquake Engineering* **7:2**, 160-179
- Imazu, M. and Fukutake, K. (1986). Dynamic Shear Modulas and Damping of Gravel Materials *Proc. of 21th Annual Meeting of The Japanese Geotechnical Society* 609-511.
- Kitsunezaki, T., Goto, N., Kobayashi, Y., Ikawa, T., Horike, M., Saito, T., Kuroda, T., Yamane, K. and Okuzumi, Y., (1990). Estimation of P- and S- Wave Velocities in Deep Soil Deposits for Evaluating Ground Vibrations in Earthquake. *Journal of Japan Society for Natural Disaster Science* **9:3**,1-17
- Satoh, T., (2005). Short-period level of acceleration source spectra and site responses at strong motion stations during the 2005/8/16 Miyagi-oki earthquake. *Programme and Abstracts The Seismological Society of Japan 2005, Fall Meeting*, **PM24**.
- Satoh, T., (2006a). Influence of Fault Mechanism, Depth, and Region on Stress Drops of Small and Moderate

Earthquakes in Japan. *Structural Eng./Earthquake Eng., JSCE*, **23:1**,125-134.
Sato, T., (2006b). Inversion of Q_s of Deep Sediments from Surface-to-Borehole Spectral Ratios Considering Obliquely Incident SH and SV Waves. *Bull. Seism. Soc. Am.*, **96:3**, 943-956